



**HAL**  
open science

## Mechanistic explanation of the (up to) 3 release phases of plga microparticles: monolithic dispersions studied at lower temperatures

Fahima Tamani, Celine Bassand, Mounira Hamoudi, Florence Siepmann, Juergen Siepmann

### ► To cite this version:

Fahima Tamani, Celine Bassand, Mounira Hamoudi, Florence Siepmann, Juergen Siepmann. Mechanistic explanation of the (up to) 3 release phases of plga microparticles: monolithic dispersions studied at lower temperatures. *International Journal of Pharmaceutics*, 2021, *International Journal of Pharmaceutics*, 596, pp.120220. 10.1016/j.ijpharm.2021.120220 . hal-04457733

**HAL Id: hal-04457733**

**<https://hal.univ-lille.fr/hal-04457733>**

Submitted on 29 Apr 2024

**HAL** is a multi-disciplinary open access archive for the deposit and dissemination of scientific research documents, whether they are published or not. The documents may come from teaching and research institutions in France or abroad, or from public or private research centers.

L'archive ouverte pluridisciplinaire **HAL**, est destinée au dépôt et à la diffusion de documents scientifiques de niveau recherche, publiés ou non, émanant des établissements d'enseignement et de recherche français ou étrangers, des laboratoires publics ou privés.

Research article

**Mechanistic explanation of the (up to) 3 release phases of PLGA microparticles:  
Monolithic dispersions studied at lower temperatures**

F. Tamani,<sup>°</sup> C. Bassand,<sup>°</sup> M.C. Hamoudi, F. Siepmann, J. Siepmann\*

*Univ. Lille, Inserm, CHU Lille, U1008, F-59000 Lille, France*

*°contributed equally*

*\*correspondence:*

Prof. Juergen SIEPMANN

University of Lille, College of Pharmacy, INSERM U1008

3 rue du Professeur Laguesse, 59006 Lille, France

Phone: +33-3-20964708, [juergen.siepmann@univ-lille.fr](mailto:juergen.siepmann@univ-lille.fr)

**Abstract**

The aim of this study was to better understand the underlying drug release mechanisms in poly(lactic-co-glycolic acid) (PLGA) microparticles in which the drug is dispersed in the form of tiny particles (“monolithic dispersions”). Differently sized diprophylline-loaded microparticles were prepared using a solid-in-oil-in-water solvent extraction/evaporation technique. The microparticles were characterized before and after exposure to phosphate buffer pH 7.4 at 4, 20 and 37 °C. In vitro drug release was measured from *ensembles* and *single* microparticles. GPC, DSC, SEM, gravimetric analysis, drug solubility measurements and optical microscopy were used to elucidate the importance of polymer swelling & degradation, drug dissolution and diffusion. The diprophylline was initially homogeneously distributed throughout the microparticles in the form of tiny crystals. The burst release (1<sup>st</sup> phase) was strongly temperature-dependent and likely attributable to the dissolution of drug crystals with direct surface access (potentially via tiny pores). The about constant release rate during the 2<sup>nd</sup> phase also strongly depended on the temperature. It can probably be explained by the dissolution of drug crystals in surface near regions undergoing *local* swelling. During the observation period, the 3<sup>rd</sup> (again rapid) drug release phase was only observed at 37 °C, and seems to be caused by substantial PLGA swelling throughout the entire microparticles. This phase starts as soon as a critical polymer molecular weight of about 25 kDa is reached: Significant amounts of water penetrate into the systems, dissolving the remaining diprophylline crystals and substantially increasing the mobility of the dissolved drug molecules. Thus, this study provides additional experimental evidence (obtained at lower temperatures) confirming the hypothesized root causes for drug release from PLGA microparticles containing dispersed drug particles.

**Keywords:** PLGA; microparticle; drug release mechanism; diffusion; dissolution; diprophylline

## 1. Introduction

Poly(lactic-co-glycolic acid) (PLGA)-based microparticles offer an interesting potential as parenteral controlled drug delivery systems, because they: (i) are biodegradable (avoiding the removal of empty remnants upon drug exhaust) (Acharya et al., 2010; Bragani et al., 2018; Mylonaki et al., 2018; Liu et al., 2019a), (ii) are biocompatible (Anderson et al., 1997), (iii) allow for the control of drug release during flexible periods of time (ranging from a few days up to several months) (Pradal et al., 2015; Ruan et al., 2018; Nanaki et al., 2018), and (iv) are rather easily administered (injected), compared to macroscopic implants. Since decades different types of controlled release PLGA microparticles are commercially available, in particular for the treatment of cancer. A variety of manufacturing methods can be used to prepare this type of advanced drug delivery systems, including emulsion solvent extraction/evaporation techniques, hot melt extrusion & grinding, and spray-drying (Jiang et al., 2005; Riehl et al., 2015; Arrighi et al., 2019).

Numerous types of PLGA-based microparticles have been reported in the literature, exhibiting broad ranges of drug release kinetics (Ibrahim et al., 2005; Berkland et al., 2007; Luan and Bodmeier, 2006; Wang et al., 2019a-c; Fraguas-Sanchez et al., 2020). In general, the observed drug release patterns are either mono-, bi- or tri-phasic (Fredenberg et al., 2015; Liu et al., 2019b; Fang et al., 2019). In the latter case an initial rapid drug release phase (also called “burst effect” = 1<sup>st</sup> release phase) is followed by a period with an about constant drug release rate (= 2<sup>nd</sup> release phase) and a final (again rapid) 3<sup>rd</sup> release phase (which leads to complete drug exhaust). Certain PLGA microparticles exhibit only mono- or bi-phasic drug release patterns (because all drug is released before the 2<sup>nd</sup> or 3<sup>rd</sup> release phase would set on).

It has to be pointed out that despite the steadily increasing practical importance of PLGA microparticles, the underlying mass transport mechanisms controlling drug release are often not fully understood. Thus, product optimization is generally based on time-consuming and cost-

intensive series of trial-and-error experiments. The lack of a thorough understanding of how the drug is released from PLGA microparticles can at least partially be explained by the potential complexity of the involved chemical and physical phenomena (Siepmann and Goepferich, 2001; Huang and Brazel, 2001; Blasi et al., 2005). A variety of processes might be involved, such as water diffusion, drug dissolution, drug diffusion, polymer degradation & erosion, drug-polymer interactions (e.g., plasticizing effects), polymer swelling and autocatalytic effects (Friess and Schlapp, 2002; Doty et al., 2017; Busatto et al., 2018; Wang et al., 2019a). The latter can occur, because the degradation products of PLGA are acids. Importantly, water penetrates relatively rapidly into the entire systems upon exposure to aqueous fluids. Thus, polymer degradation occurs throughout the microparticles and shorter chain acids are generated within the entire devices (“bulk erosion”). The rate at which the acids are generated can be higher than the rate at which they diffuse out into the surrounding release medium, or at which they are neutralized by bases from the environment, diffusing into the microparticles (Brunner et al., 1999; Fu et al., 2000; Schaedlich et al., 2014; Liu et al., 2019c). Consequently, the pH within PLGA microparticles might locally significantly drop. Since ester hydrolysis is catalyzed by protons, this can lead to autocatalysis: Polymer degradation is accelerated. The importance of this effect has been reported to depend on the microparticle size and porosity, both affecting the rates at which acids and bases diffuse into and out of the systems (Grizzi et al., 1995; Klose et al., 2006).

Based on drug release and swelling studies of *single* PLGA microparticles (instead of *ensembles* of microparticles), it has recently been hypothesized that the role of PLGA swelling is often underestimated (Gasmi et al., 2015a,b; 2016; Tamani et al., 2019a,b). This is also true for PLGA implants (Bode et al., 2019a,b). In brief, it has been suggested that PLGA swelling is not negligible, as often assumed, but in contrast plays an “orchestrating role” for the control of drug release from PLGA-based drug delivery systems. The theory is as follows: Upon contact

with aqueous body fluids (e.g., upon s.c. or i.m. injection), water penetrates relatively rapidly into the entire PLGA microparticles. However, at this stage, the polymer is rather hydrophobic and the macromolecules are highly entangled. This limits the amounts of water that can enter the microparticles. Nevertheless, the entire systems are wetted (often within less than 1 d) and polyester bond cleavage starts throughout the microparticles (Burkersroda et al., 2002). Consequently, the polymer chains become shorter with time, and new –OH and –COOH groups are created throughout the microparticles. This renders the polymeric matrices more and more hydrophilic with time. Also, the degree of polymer chain entanglement decreases (the chains becoming shorter). In addition, the low molecular weight degradation products are water soluble (e.g., lactic acid and glycolic acid). Thus, a steadily increasing osmotic pressure is built up within the microparticles, attracting more water into the system. At a certain time point (e.g., when a critical polymer molecular weight is reached), the polymeric matrices become sufficiently hydrophilic to allow for the penetration of *significant* amounts of water into the system. In addition, the mechanical stability of the polymer network becomes insufficient to withstand the generated osmotic pressure: *Substantial* system swelling sets on, fundamentally altering the conditions for drug release: Important amounts of water are available for drug dissolution and the mobility of *dissolved* drug molecules/ions is significantly increased. Consequently, the release rate increases. This is likely the root cause for the onset of the final (e.g., 3<sup>rd</sup>) release phase.

Recently, Tamani et al. (2019a,b) proposed that in the case of diprophylline-loaded PLGA microparticles (in which the drug is homogeneously dispersed in the form of tiny crystals throughout the matrix) the initial burst release and the 2<sup>nd</sup> release phase (with an about constant release rate) can be explained by the occasional release of parts of the drug “having direct access” to the microparticles’ surface or being located in surface near regions undergoing *local* swelling before the onset of the fundamental swelling of the entire system. Importantly, every

microparticle has its own structure and its “own way” to release the drug. If a drug crystal has direct surface access from the beginning (eventually via pores/channels), it will rapidly dissolve and the dissolved drug molecules will be rapidly released. The sum of such events likely constitutes the burst release. With time, certain PLGA regions (especially surface near regions) undergo *local* swelling (prior to the onset of substantial polymer swelling *throughout the entire* system). If a drug crystal is located in such a region, it gets into contact with significant amounts of water, dissolves and the dissolved drug molecules/ions rather rapidly diffuse through the swollen PLGA. The about *constant* release rate from *ensembles* of microparticles during the 2<sup>nd</sup> release phase is likely the sum of numerous *occasional individual* release events of this type, which occur randomly in time. However, the above described release mechanisms are hypotheses, which are so far based on a limited number of experiments only, which were conducted under specific conditions, in particular at only one single temperature: 37 °C.

The aim of the present study was to provide further experimental evidence allowing to better understand the underlying drug release mechanisms from PLGA microparticles, altering the temperature of the release medium: In addition to 37 °C, the systems were also exposed to phosphate buffer pH 7.4 at 20 and 4 °C. The idea was to potentially slow down key phenomena, such as polymer degradation. Thus, the resulting release kinetics might (or might not) substantially change. Potential changes were to be explained based on a thorough characterization of the microparticles before and after exposure to the release medium at the different temperatures. In particular, the release and swelling behavior of *single* microparticles as well as the degradation and release kinetics of *ensembles* of microparticles were to be monitored. Differently sized microparticle batches were prepared, with mean diameters of 63 +/- 19, 113 +/- 41 and 296 +/- 95 µm. Please note that in this study it was technically not possible to monitor *single small* microparticles (but only larger systems). The assumption is that the underlying drug release mechanisms in small, medium-sized and large microparticles

are not *fundamentally* different, given the fact that there were no visible signs for differences in their inner & outer structure and composition. This does not mean that the relative importance of specific phenomena might not depend on the system size (as discussed in more detail in this article). In addition to drug release measurements (from *ensembles* of microparticles and *single* microparticles), the systems were also characterized by optical and Scanning Electron Microscopy (SEM), Differential Scanning Calorimetry (DSC), Gel Permeation Chromatography (GPC), gravimetric analysis as well as drug content and drug solubility measurements.

Diprophylline has been chosen in this study as a freely water-soluble model drug. Please note that other drugs can be expected to behave differently, depending on their specific physico-chemical properties. Thus, (as always) caution should be paid when drawing conclusions for different types of PLGA microparticles. However, the authors believe that the hypothesized drug release mechanisms are valid also for many other drugs, especially water-soluble compounds with a limited affinity to PLGA, forming “monolithic dispersions”.

## **2. Materials and methods**

### *2.1. Materials*

Poly (D,L lactic-co-glycolic acid) (PLGA; Resomer RG 504H; 50:50 lactic acid:glycolic acid; Evonik, Darmstadt; Germany); diprophylline (BASF, Ludwigshafen, Germany); polyvinyl alcohol (Mowiol 4-88; Sigma-Aldrich, Steinheim, Germany); acetonitrile and dichloromethane (VWR, Fontenay-sous-Bois, France); tetrahydrofuran (HPLC grade; Fisher Scientific, Illkirch, France).



## 2.2. *Microparticle preparation*

Drug-loaded microparticles were prepared using a solid-in-oil-in-water (S/O/W) solvent extraction/evaporation technique. “Small”, “medium-sized” and “large” microparticles were obtained, adapting the formulation and processing parameters accordingly (as indicated in the following in brackets, please be aware of the order). Appropriate amounts of diprophylline (204, 125 or 101 mg) and PLGA (900, 834 or 910 mg) were dispersed/dissolved (the drug was at least partially dispersed in the form of tiny particles, the polymer was dissolved) in 10, 6 or 4 mL dichloromethane. The organic phase was emulsified into 2.5 L of an outer aqueous polyvinyl alcohol solution (0.25% w/w) under stirring (2000, 1500 or 1000 rpm, Eurostar power-b; Ika, Staufen, Germany) for 30 min. Upon solvent exchange the PLGA precipitated, trapping the drug. The formed microparticles were hardened by adding 2.5 L of the same outer aqueous polyvinyl alcohol solution (0.25%) and further stirring at 700 rpm (Eurostar power-b) for 4 h. The microparticles were separated by filtration (Nylon filter, 0.45  $\mu\text{m}$ , 13 mm; GE Healthcare Life Sciences Whatman, Kent, UK), washed with de-mineralized water and subsequently freeze-dried (freezing at  $-45^{\circ}\text{C}$  for 1 h 45 min, primary drying at  $-40^{\circ}\text{C}$  and 0.07 mbar for 35 h, and secondary drying at  $+20^{\circ}\text{C}$  and 0.0014 mbar for 35 h) (Christ Epsilon 2-4 LSC+; Martin Christ, Osterode, Germany).

## 2.3. *Microparticle characterization*

### 2.3.1. *Microparticle morphology and size*

Microparticle sizes were determined by optical microscopy: Pictures were taken using an Axiovision Zeiss Scope-A1 microscope, equipped with an AxioCam ICc1 camera and the Axiovision Zeiss Software (Carl Zeiss, Jena, Germany). For *ensembles* of microparticles, each measurement included 200 particles. Mean values +/- standard deviations are reported.

### 2.3.2. Practical drug loading

The practical drug loading was determined by dissolving approximately 5 mg microparticles in 5 mL acetonitrile, followed by filtration (PTFE syringe filters, 0.45  $\mu\text{m}$ ; GE Healthcare, Kent, UK). The drug content was determined by HPLC-UV analysis [Thermo Fisher Scientific Ultimate 3000 Series HPLC, equipped with a LPG 3400 SD/RS pump, an auto sampler (WPS-3000 SL) and a UV-Vis detector (VWD-3400RS); Thermo Fisher Scientific, Waltham, USA]. A reversed phase column Polar C18 (Luna Omega 3  $\mu\text{m}$ ; 150 x 4.6 mm; Phenomenex, Le Pecq, France) was used. The mobile phase was a mixture of acetate buffer (0.01 M, pH 4.5): acetonitrile (65:35, v:v). The detection wavelength was 274 nm and the flow rate 1 mL/min. Five  $\mu\text{L}$  samples were injected. The standard curve covered the range of 0.1 to 50  $\mu\text{g/mL}$ . Each experiment was conducted in triplicate. Mean values  $\pm$  standard deviations are reported.

### 2.3.3. Drug release measurements from *ensembles* of microparticles

Ten mg microparticle samples were placed into plastic tubes (Safe-lock tubes 2.0 mL, Eppendorf, Hamburg, Germany) filled with 2 mL phosphate buffer pH 7.4 (USP 42). The tubes were placed into a horizontal shaker at 37°C & 80 rpm or at 20°C & 80 rpm (GFL 3033; Gesellschaft fuer Labortechnik, Burgwedel, Germany) or into a refrigerator at 4°C (0 rpm), as indicated. At predetermined time points, 1.5 mL samples were withdrawn (replaced with fresh medium), filtered (PTFE syringe filters, 0.45  $\mu\text{m}$ ; GE Healthcare) and analyzed for their drug contents by HPLC-UV analysis, as described above. Each experiment was conducted in triplicate. Mean values  $\pm$  standard deviations are reported. Sink conditions were provided throughout all experiments.

In addition, the pH of the release medium was measured at pre-determined time points using a pH meter (InoLab pH Level 1; WTW, Weilheim, Germany) (n=3). Mean values  $\pm$  standard deviations are reported.

#### 2.3.4. Drug release measurements from *single* microparticles

Diprophylline release from *single* microparticles was monitored in 96- well standard microplates (Tissue culture plate 96 well; Carl Roth, Karlsruhe, Germany) as follows: One microparticle was introduced into each well, which was filled with 100  $\mu$ L phosphate buffer pH 7.4 (USP 42) and closed with a cap (Simport Scientific, Beloeil, Quebec). The well microplates were placed into a horizontal shaker at 20°C & 80 rpm (GFL 3033). At pre-determined time points, 50  $\mu$ L samples were withdrawn (replaced with fresh medium) using a Hamilton syringe (Microlite #710, 100  $\mu$ L; Hamilton, Bonaduz, Switzerland) and analyzed for their drug contents by HPLC-UV, as described above (in this case the standard curve covered the range of 0.025 to 5  $\mu$ g/mL).

#### 2.3.5. Swelling of *single* microparticles

Microparticles were treated as for the drug release studies from *single* microparticles. At pre-determined time points, pictures were taken using an Axiovision Zeiss Scope-A1 microscope and the Axiovision Zeiss Software (Carl Zeiss) to monitor changes in the microparticles' diameter.

Furthermore, dynamic changes in the microparticles' wet mass were determined as follows: At pre-determined time points, samples were carefully withdrawn and excess water removed using Kimtech precision wipes (Kimberly-Clark, Rouen, France). The microparticles' wet mass was measured using an ultra-microbalance (XPR6U; Mettler-Toledo, Greifensee, Switzerland).

### 2.3.6. Differential Scanning Calorimetry (DSC)

DSC thermograms of raw materials (as received: diprophylline, PLGA) and of microparticles were recorded with a DSC1 Star system (Mettler Toledo, Greifensee, Switzerland). Approximately 5 mg samples were heated in sealed aluminum pans from 10 °C to 120°C, cooled to -70 °C and reheated to 120 °C at a rate of 10 °C/min. The indicated glass temperatures (T<sub>gs</sub>) were obtained from the second heating cycles. Each experiment was conducted in triplicate. Mean values +/- standard deviations are reported.

### 2.3.7. Scanning Electron Microscopy (SEM)

The external morphology of microparticles was studied using a JEOL Field Emission Scanning Electron Microscope (JSM-7800F, Tokyo, Japan). Samples were fixed with a ribbon carbon double-sided adhesive and covered with a fine chrome layer. Microparticles were observed before and after exposure to the release medium. In the latter case, the microparticles were treated as for the drug release studies from *ensembles* of microparticles (described above). At pre-determined time points, samples were withdrawn and freeze-dried (as described above).

### 2.3.8. Gel Permeation Chromatography (GPC)

Microparticles were treated as for the drug release studies from *ensembles* of microparticles. At pre-determined time points, samples were withdrawn, freeze-dried for 3d (as described above) and the lyophilisates were dissolved in tetrahydrofuran (at a concentration of 3 mg/mL). The average polymer molecular weight (M<sub>w</sub>) of the PLGA in the samples was determined by GPC (Alliance, refractometer detector: 2414 RI, separation module e2695, Empower GPC software; Waters, Milford, USA), using a Phenogel 5 µm column (which was kept at 35°C, 7.8 × 300 mm; Phenomenex). The injection volume was 50 µL. Tetrahydrofuran

was the mobile phase (flow rate: 1 mL/min). Polystyrene standards with molecular weights between 1480 and 70,950 Da (Polymer Laboratories, Varian, Les Ulis, France) were used to prepare the calibration curve.

#### *2.4. Drug solubility measurements*

Excess amounts of drug (as received) were exposed to 25 mL phosphate buffer pH 7.4 in brown glass flasks and horizontally shaken at 37°C or 20 °C at 80 rpm (GFL 3033), or placed in a refrigerator at 4 °C (and regularly shaken manually). At pre-determined time points, samples were withdrawn, immediately filtered (PTFE syringe filters, 0.45 µm; GE Healthcare) and diluted. The drug contents of the samples were determined by HPLC-UV, as described above. Samples were withdrawn until equilibrium was reached. Each experiment was conducted in triplicate, mean values +/- standard deviations are reported.

### **3. Results and discussion**

In all cases, spherical particles were obtained, with mean sizes (+/- standard deviation) of 63 +/- 19, 113 +/- 41 and 296 +/- 95 µm for “small”, “medium-sized” and “large” microparticle batches, respectively. SEM pictures revealed no signs for noteworthy external porosity prior to exposure to the release medium (top row in Figure 1). But please note that very small pores might not be visible, since the surfaces were covered with a fine chrome layer prior to the analysis. The practical drug loadings were about 5-7 % (4.8 +/- 0.3, 5.8 +/- 0.6 and 6.7 +/- 0.4 %) and the glass transition temperatures (T<sub>g</sub>s) about 46-47 °C (46.8 +/- 0.1, 46.3 +/- 0.3 and 46.4 +/- 0.4 °C). It has recently been reported that the T<sub>g</sub> of the polymer raw material (as received) was 47.0 +/- 0.2 °C (Tamani et al., 2019a). Hence, diprophylline is not acting as a

plasticizer for PLGA. Furthermore, X-ray diffraction and SEM pictures of cross-sections of these microparticles revealed numerous tiny drug crystals, which are distributed throughout the systems (Tamani et al., 2019a). Thus, probably only minor amounts of the hydrophilic diprophylline are *dissolved* within the much more hydrophobic PLGA, most of the drug is likely *dispersed* in the form of tiny particles within the PLGA matrix. The absence of plasticizing effects and the fact that “monolithic *dispersions*” (and not “monolithic *solutions*”) were obtained suggest that the affinity between diprophylline and PLGA is limited.

### 3.1. Drug release from *ensembles* of microparticles

Figure 2 shows the resulting diprophylline release kinetics from the investigated PLGA microparticles in phosphate buffer pH 7.4 at 37 °C (top), 20 °C (middle) and 4 °C (bottom). Please note that the systems were agitated (80 rpm) at 37 and 20 °C, but not at 4 °C. However, it has been shown that the impact of agitation (0 vs. 80 rpm) on drug release from these microparticles is limited at 37 °C (Tamani et al., submitted). The mean particle sizes (+/- SD) are indicated in the diagrams. “Small”, “medium-sized” and “large” microparticle batches are marked in red, black and orange, respectively. At 37 °C, also a zoom on the first 3 weeks is shown.

Interestingly, the following observations can be made:

- The drug release rate increased with increasing temperature, irrespective of the microparticle size.
- At all temperatures, the release rate generally increased with decreasing microparticle size.
- At 37 °C, 3-phasic drug release was observed, irrespective of the microparticle size: An initial rapid drug release phase (“burst”) was followed by a 2<sup>nd</sup> release phase with an about constant release rate, and a final (again rapid) 3<sup>rd</sup> release phase (leading to complete drug exhaust).

- At 20 and 4 °C, the drug release patterns were only bi-phasic in the observation period (100 d), irrespective of the microparticle size: A “burst” release was followed by a 2<sup>nd</sup> release phase with an about constant release rate. Please note that at the end of the observation period, diprophylline release was far from being complete at these temperatures, especially at 4 °C (e.g., less than about 30 % diprophylline was released at this time point). It can be hypothesized that at later time points, also a 3<sup>rd</sup> release phase will likely be observed at these temperatures. Actually, looking at the orange curve in the middle of Figure 2 (20 °C, “large” microparticles), such a final rapid release phase might just begin after 90 – 100 d.
- The slopes of the 2<sup>nd</sup> release phases (with about constant release rates) strongly increase with increasing temperature.
- The importance of the burst release (“1<sup>st</sup> phase”) increases with increasing temperature.

To better understand these phenomena and tendencies, the degradation of the polymer upon exposure to the release medium as well as potential changes of the external morphology and pH of the surrounding bulk fluids were monitored. Also, the swelling and drug release kinetics of *single* microparticles were measured at the different temperatures.

### 3.2. Polymer degradation, bulk fluid pH and outer microparticle morphology

Figure 3 shows the decrease in polymer molecular weight (Mw) of the diprophylline-loaded PLGA microparticles as a function of the exposure time to phosphate buffer pH 7.4 at the different temperatures. The systems were treated as for the in vitro drug release studies from *ensembles* of microparticles (described above). Clearly, the polymer degradation rate substantially increased with increasing temperature: At 37 °C, the polymer molecular weight decreased from about 48 kDa to only about 8 kDa in the first 3 weeks. At 20 °C, the Mw decreased only to about 41 kDa in the same time period, and at 4 °C there was virtually no

change in the polymer molecular weight in this observation period. This can be explained by the fact that the rate of the hydrolytic ester bond cleavage strongly depends on the temperature.

The dynamic changes in the pH of the release medium upon exposure of *ensembles* of diprophylline-loaded PLGA microparticles to phosphate buffer pH 7.4 at different temperatures are illustrated in Figure 4. The systems were treated as for the *in vitro* drug release studies described above. Clearly, the pH of the surrounding bulk fluid remained about constant during the observation periods in all cases: at all temperatures and for all microparticle sizes. Thus, under the given conditions, potential acidifications of the *surrounding bulk fluid* due to the leaching of short chain acids (PLGA degradation products) from the microparticles do not seem to play a noteworthy role in these time periods. Please note that this does not exclude potential autocatalytic effects *within* the microparticles.

The SEM pictures in Figure 1 show surfaces of the microparticles after 0, 3, 7 and 10 d exposure to the release medium at 20 °C. Please note that after exposure to the phosphate buffer the microparticles had to be dried prior to the analysis (in this study they were freeze-dried). Thus, artefact creation cannot be excluded. As it can be seen, no signs for pore formation were observed. The same is true for microparticles which were exposed to the release medium at 4 °C for up to 10 d (Tamani et al., submitted). In contrast, when the microparticles were exposed to phosphate buffer pH 7.4 at 37 °C for 10 d, surface pores became visible (Tamani et al., 2019a), reflecting substantial PLGA degradation (please see above).

### 3.3. Drug release from and swelling of *single* microparticles

Figure 5 shows optical microscopy pictures of the investigated microparticles upon exposure to phosphate buffer pH 7.4 at 20 °C for up to 74 d. The initial microparticle diameters are indicated on the left-hand side. Importantly, no major changes were observed in this time period. This is in contrast to *substantial* microparticle swelling that was reported upon exposure



of the same microparticles to the same release medium, but at 37 °C (Tamani et al., 2019a): At body temperature, substantial microparticle swelling set on after about 1 week, irrespective of the microparticle size. This can be explained by the difference in the PLGA degradation rates (Figure 3) at these temperatures, and it has important consequences for drug release. Figure 6 shows the dynamic changes in the diameters of individual microparticles and in the latter's wet mass as a function of the exposure time to phosphate buffer at 20 °C. The results are consistent with the optical microscopy pictures in Figure 5 and indicate the absence of *substantial* microparticle swelling under the given conditions in the observation period. Please note that at  $t = 100$  d, eventually the beginning of important microparticle swelling is visible in specific cases (e.g., the diameters of certain microparticles might start to significantly increase, pink curves in the top diagram in Figure 6). This would coincide with the potential onset of a 3<sup>rd</sup> drug release phase observed for the “larger” microparticles (orange curve in Figure 2). At 4 °C, microparticle swelling was very much limited during the first 100 d (Tamani et al., submitted).

Figure 7 shows the swelling kinetics of *single* microparticles together with their drug release kinetics in the same diagrams upon exposure to phosphate buffer pH 7.4 at 20 °C. The left y-axes refer to drug release, the right y-axes to changes in the systems' diameters. The initial particle size (before exposure to the release medium) is indicated at the top of each diagram. As it can be seen, each microparticle behaved differently, “releasing the drug in its own way”. In some cases, especially at lower initial microparticle sizes, more or less important *portions* of the drug were released in rather short time periods (marked by red stars). In other cases, drug release was very limited during the observation period. Figure 8 shows all the individual microparticle release profiles (at 20 °C) in one diagram. As it can be seen, many microparticles do not release any diprophylline to a noteworthy extent during the observation period, whereas others release parts of their drug load rather arbitrarily at different time points and to different extents. These differences in the behaviors of the *individual* microparticles can

be attributed to the unique properties of each system: Every microparticle has its own specific composition, geometry, dimensions as well as outer and inner structure. For example, the distribution of the tiny drug crystals within the polymer matrices is unique in each case. Certain microparticles contain drug particles with direct surface access, others do not. In certain microparticles, some of the embedded drug crystals are located close to the surface, in others this is not the case. All these individual characteristics can be expected to affect the resulting drug release rate, as explained in more detail in the following.

### 3.4. Hypothesized drug release mechanisms

Based on the above described experimental observations, the following drug release mechanisms are hypothesized for the different release phases:

The initial “burst” release (= 1<sup>st</sup> phase) is caused by the release of drug crystals with direct surface access from the beginning. This does not mean that a part of the respective drug crystal is necessarily *directly* located at the system’s surface: Also an access via a tiny pore/channel can allow for rapid drug crystal dissolution and subsequent diffusion through the pore/channel. The scheme at the top of Figure 9 illustrates this release mechanism. Please note that such pores might be very small and not visible on SEM pictures (e.g., due to the sputtering of the chrome layer in this study). Previously, *single* microparticle release studies evidenced that some of the microparticles release parts of their drug loading right from the beginning upon exposure to phosphate buffer pH 7.4 at 37 °C (Tamani et al., 2019a). In the present study, none of the investigated *single* microparticles showed such a release behavior at 20 °C (Figure 7). This is consistent with the observed drug release kinetics from *ensembles* of microparticles at 20 °C (diagram in the middle of Figure 2): As it can be seen, the “burst effect” was very much limited in the case of “medium-sized” and “large” microparticles (black and orange curves). Only in the case of “small” microparticles (red curve), an important burst release was observed

at this temperature. But the release from *single* “small” microparticles could not be monitored in this study, for technical reasons. The fact that the “initial burst release” phase is much more important in the case of small microparticles compared to larger microparticles can be explained as follows: The total surface area of numerous small microparticles is much higher than the surface area of much fewer, larger microparticles (the sum of the *volumes* of the two populations being equal). Consequently, the probability that a drug crystal has “direct surface access” (eventually via a tiny pore/channel) is much higher in the case of smaller microparticles. This is schematically illustrated in Figure 10.

Interestingly, the importance of the initial burst release phase also strongly depends on the temperature: As it can be seen in Figure 2, the burst release was much more pronounced at 37 °C compared to 20 °C and 4 °C. This cannot solely be explained by differences in the drug’s diffusivity or solubility at the investigated temperatures: Such differences could explain a decrease in the release *rate* during this time period, but not a difference in the *extent* of the burst release (here, the “height” of the beginning of the “2<sup>nd</sup> release phase”) (perfect sink conditions being provided in the well agitated bulk fluid throughout the observation period). According to Fick’s law, the rate of drug diffusion depends on the diffusion coefficient (which is a measure for the mobility of the drug) and the concentration difference (which might locally be limited by the drug solubility). But the amount of drug which is in direct contact with the microparticles’ surface from the beginning is not depend on the temperature (it depends on the microparticle structure). Consequently, the fact that the *extent* of the initial burst release from the microparticles strongly depends on the temperature likely indicates that pore closure effects as described by the group of Steven Schwendeman (Huang et al., 2005; Kang and Schwendeman 2007) are of importance: Upon contact with aqueous media, limited amounts of water rapidly penetrate into the entire systems and polymer degradation starts throughout the microparticles (“bulk erosion”). These limited amounts of water can be expected to also lead to

limited PLGA swelling, closing tiny pores/channels, which gave some of the drug crystals “direct surface access” at early time points. Once the pores/channels are closed, the “burst release” ends. As long as the pores/channels are “open”, drug crystals in contact with such openings can (at least partially) dissolve, and the dissolved drug molecules can rather rapidly be released. At 37 °C, the diffusivity of the drug in the water-filled channels can be expected to be higher than at 20 and 4 °C. In addition, at 37 °C, the solubility of diprophylline in the release medium is higher than at 20 and 4 °C: 169 +/- 8 compared to 128 +/- 11 and 79 +/- 6 mg/mL, respectively. The higher mobility of the drug and the higher drug solubility (leading to higher concentration gradients - the driving forces for diffusion) result in higher drug release rates during the “burst release phase” at higher temperatures. Importantly, the duration of this burst phase is limited due to pore closure. Consequently, lower release rates lead to lower amounts of drug release. In brief, at 37 °C the drug can more easily dissolve and more rapidly diffuse through the “open” pores/channels compared to 20 and 4 °C during this limited time period. Once the pores are “closed” by (limited) PLGA swelling, the burst release phase is terminated. Please note that the temperature might also affect the rate of the PLGA swelling and, thus, alter the time period during which the pores are open, e.g. slower swelling at lower temperatures might lead to longer burst release periods. However, the experimentally measured drug release kinetics (Figure 2) indicate that such effects do not seem to play a noteworthy role in the investigated systems.

The 2<sup>nd</sup> release phase can probably be attributed to the occasional release of tiny drug crystals, which are located in “surface near” regions. As illustrated in the cartoon in the middle of Figure 9, in surface near regions the polymer can be expected to locally swell before the entire system starts to substantially swell. Experimental evidence (optical microscopy pictures) for this phenomenon were recently reported for the investigated microparticles upon exposure to phosphate buffer pH 7.4 at 37 °C (Tamani et al., 2019a). At 20 °C this phenomenon is much

less pronounced, because PLGA degradation is much slower (Figure 3). This surface-near polymer swelling can be attributed to the high water amounts the microparticle surface is in contact with: These high concentrations of water likely *locally* accelerate ester bond cleavage as well as water penetration into these regions. In the cartoon in the middle of Figure 9, such swollen PLGA regions are marked in light grey, the only slightly hydrated PLGA regions are marked in dark grey. As long as a drug crystal is surrounded by essentially non-swollen polymer, the amount of water available for dissolution is very much limited and the mobility of dissolved diprophylline molecules is low. However, once the neighborhood of a drug crystal undergoes substantial swelling, much higher amounts of water get into contact with the crystal and dissolved drug molecules can much more easily diffuse out through the swollen system. Such an event can be expected to lead to rather rapid release of the respective drug crystal (or network of crystals, if they are interconnected by pores or channels). This type of phenomenon was likely observed with some of the microparticles shown in Figure 7: The red stars highlight “sudden” partial drug release events. The size of the drug crystal (or network of interconnected drug crystals) can be expected to determine the “height of the respective release step”. Importantly, the time points of these events are *randomly* distributed. Thus, a population of numerous microparticles shows an about *constant* drug release rate. This is consistent with the “2<sup>nd</sup> release phases” from *ensembles* of microparticles shown in Figure 2. The fact that the time points of sudden partial drug release events are rather randomly distributed throughout the duration of the 2<sup>nd</sup> drug release phase can be explained by the homogeneous distribution of the drug crystals throughout the microparticles [as evidenced by SEM pictures of cross-sections, (Tamani et al., 2019a)] and an about constant rate at which the surface near swelling zone grows with time. Please note that this theory is also consistent with the experimentally observed slight and about constant increase in the microparticles’ diameter with time during the 2<sup>nd</sup> drug release phase (Figure 6, 20 °C).

Importantly, the slope of the 2<sup>nd</sup> drug release phase strongly depended on the temperature (Figure 2): The release rate clearly increased when increasing the temperature from 4 to 20 to 37 °C. This can be explained by the more rapid local swelling of the PLGA, as evidenced for instance by optical microscopy, comparing the results obtained in this study at 20 °C (Figure 5) with the results obtained by Tamani et al. (2019a, submitted) at 37 and 4 °C. Again, this is likely attributable to the temperature dependent PLGA degradation rate (Figure 3).

Please note that in the present case, drug dissolution and subsequent *diffusion through the continuous and essentially non-swollen* PLGA matrix is likely to be negligible, although the polymer can be expected to be in the rubbery state during most of the release period: Upon exposure to the aqueous bulk fluid, limited amounts of water rapidly penetrate into the entire system (initiating polymer degradation throughout the microparticles, “bulk erosion”) and decrease the glass transition temperature of PLGA by about 10-15 °C (Faisant et al., 2002; Blasi et al., 2005). The fact that the contribution of drug diffusion through the essentially non-swollen, but rubbery polymer matrix is negligible in the present case can at least in part be explained by the limited affinity between diprophylline and PLGA: As discussed above, the absence of a plasticizing effect of the drug and the observation that most of the diprophylline is *dispersed* in the polymer matrix in the form of tiny crystals (and not dissolved) indicates limited drug-polymer affinity. Please note that in the case of other drugs, exhibiting a high affinity to PLGA (and forming “monolithic solutions”), the underlying drug release mechanisms are likely different.

The 3<sup>rd</sup> release phase can be explained by the onset of *substantial polymer swelling throughout the entire microparticles* once a critical polymer molecular weight is reached. Initially, the PLGA chains are rather hydrophobic and highly entangled. This limits the water penetration into the system at early time points. With time the polymer chains are cleaved into

shorter fragments throughout the system. The polymer molecular weight decreases (Figure 3), and new –OH and –COOH groups are created, rendering the system more and more hydrophilic. Also, the degree of polymer chain entanglement decreases. In addition, water-soluble degradation products create a continuously increasing osmotic pressure within the microparticles. As soon as a certain, critical PLGA Mw threshold is reached, substantial amounts of water are driven into the system, allowing for the dissolution of the drug crystals. This is illustrated in the cartoon at the bottom of Figure 9. Importantly, the mobility of the dissolved drug molecules in the substantially swollen PLGA is rather high, resulting in the onset of the 3<sup>rd</sup> (again rapid) drug release phase, leading to complete drug exhaust. It is hypothesized that this substantial entire system swelling is the root cause for the onset of the 3<sup>rd</sup> drug release phase and that system erosion (dry mass loss) is a *consequence* (and not a cause): The important amounts of water penetrating into the system at this stage allow the water-soluble polymer degradation products to dissolve and diffuse out (as this is the case for the water-soluble drug). The resulting loss of drug and degradation products is reflected in the dry mass loss of the system (erosion).

As it can be seen at the top of Figure 1 on the right-hand side, this 3<sup>rd</sup> drug release phase set on after about 1 week exposure to the release medium at 37 °C. This corresponds to a PLGA polymer molecular weight of about 25 kDa (top of Figure 3). It has recently been reported that substantial system swelling was observed once a polymer molecular weight of about 20 kDa was reached in PLGA microparticles loaded with caffeine (Tamani et al., 2019a), dexamethasone (Gasmi et al., 2015a) and prilocaine (Gasmi et al., 2015b). The difference in the threshold values in those studies compared to the present investigation is not fully understood. At 20 and 4 °C, the PLGA degradation is much slower (Figure 3) and during the observation periods the critical Mw threshold value was not reached at these temperatures. Consequently, substantial microparticle swelling and the 3<sup>rd</sup> release phase did not yet set on.

However, please note that after 90-100 d exposure to the release medium at 20 °C, eventually the beginning of the onset of the 3<sup>rd</sup> release phase also at this temperature might be visible for larger microparticles, e.g. in Figure 2, 6 and 8.

#### 4. Conclusion

The results obtained in this study at 37, 20 and 4 °C confirm the hypothesized drug release mechanisms from PLGA-based microparticles containing dispersed drug particles (here diprophylline crystals) (“monolithic dispersions”): The burst release can likely be attributed to the release of drug crystals with direct surface access from the beginning (potentially through tiny pores). The 2<sup>nd</sup> release phase probably results from the random dissolution of (eventually interconnected) drug crystals located in surface near regions undergoing *local* swelling. The 3<sup>rd</sup> release phase is due to substantial PLGA swelling *throughout* the entire microparticles, resulting in significant amounts of water available for drug dissolution and elevated mobility of the dissolved drug molecules in the highly swollen polymer.

It will be interesting to study different types of PLGA microparticles in the future, e.g. loaded with drugs which can dissolve in the polymer forming “monolithic *solutions*”. In these cases, also drug transport through essentially non-swollen, rubbery PLGA might be of importance, especially in the case of drugs acting as plasticizers for PLGA.

A thorough mechanistic understanding of how this type of advanced drug delivery systems works can be helpful to facilitate device optimization, reducing the number of trial-and-error studies.

#### Acknowledgements



This project has received funding from the Interreg 2 Seas programme 2014-2020, co-funded by the European Regional Development Fund under subsidy contract 2S01-059\_IMODE. The authors are very grateful for this support. They would also like to thank Mr. A. Fadel from the “Centre Commun de Microscopie” of the University of Lille (“Plateau technique de la Federation Chevreul CNRS FR 2638”) as well as Mr. J. Verin from the INSERM U1008 research group at the University of Lille for their valuable technical help with the SEM pictures.

**Conflict of interests**

The Editor-in-Chief of the journal is one of the co-authors of this article. The manuscript has been subject to all of the journal's usual procedures, including peer review, which has been handled independently of the Editor-in-Chief.

## References

- Acharya, G., Shin, C.S., Vedantham, K., McDermott, M., Park, K. A study of drug release from homogeneous PLGA microstructures. *J. Control. Release.* 146 (2010) 201-206.
- Anderson, J.M., Shive, M.S. Biodegradation and biocompatibility of PLA and PLGA microspheres. *Adv. Drug Deliv. Rev.* 28 (1997) 5-24.
- Arrighi, A., Marquette, S., Peerboom, C., Denis, L., Amighi, K. Development of PLGA microparticles with high immunoglobulin G-loaded levels and sustained-release properties obtained by spray-drying a water-in-oil emulsion. *Int. J. Pharmaceut.* 566 (2019) 291-298.
- Berkland, C., Pollauf, E., Raman, C., Silverman, R., Kim, K., Pack, D.W. Macromolecule Release from Monodisperse PLG Microspheres: Control of Release Rates and Investigation of Release Mechanism. *J. Pharm. Sci.* 96 (2007) 1176-1191.
- Blasi, P., D'Souza, S.S., Selmin, F., DeLuca, P.P. Plasticizing effect of water on poly (lactide-co-glycolide). *J. Control. Release.* 108 (2005) 1-9.
- Blasi, P., Schoubben, A., Giovagnoli, S., Perioli, L., Ricci, M., Rossi, C. Ketoprofen poly (lactide-co-glycolide) physical interaction. *AAPS. PharmSciTech.* 8 (2007) 78-85.
- Bode, C. Kranz, H., Fizez, A., Siepmann, F. Siepmann, J. Often neglected: PLGA/PLA swelling orchestrates drug release - HME implants. *J. Control. Release.* 306 (2019a) 97-107.
- Bode, C. Kranz, H., Siepmann, F. Siepmann, J. Coloring of PLGA implants to better understand the underlying drug release mechanisms. *Int. J. Pharmaceut.* 569 (2019b) 118563.
- Bragagni, M., Gil-Alegre, M.E., Mura, P., Cirri, M., Ghelardini, C., Mannelli, L.D.C. Improving the therapeutic efficacy of prilocaine by PLGA microparticles: Preparation, characterization and in vivo evaluation, *Int. J. Pharmaceut.* 547 (1-2) (2018) 24-30.

- Brunner, A. Maeder, K., Goepferich, A. pH and osmotic pressure inside biodegradable microspheres during erosion. *Pharm. Res.* 16 (1999) 847-853.
- Busatto, C., Pessoa, J., Helbling, I., Luna, J., Estenoz, D. Effect of particle size, polydispersity and polymer degradation on progesterone release from PLGA microparticles: Experimental and mathematical modelling, *Int. J. Pharmaceut.* 536 (2018) 360-369.
- Doty, A.C., Weinstein, D.G., Hirota, K. (...) Schwendeman, S.P. Mechanisms of in vivo release of triamcinolone acetonide from PLGA microspheres, *J. Control. Release.* 256 (2017) 19-25.
- Faisant, N., Siepmann, J., Benoit, J.P., 2002. PLGA-based microparticles: elucidation of mechanisms and a new, simple mathematical model quantifying drug release. *Eur. J. Pharm. Sci.* 15, 355–366.
- Fang, Y., Zhang, N., Li, Q., (...) Pan, W. Characterizing the release mechanism of donepezil-loaded PLGA microspheres in vitro and in vivo, *J. Drug. Deliv. Sci. Technol.* 51 (2019) 430-437.
- Fraguas-Sanchez, A.I., Fernandez-Carballido, A., Simancas-Herbada, R., Martin-Sabroso, C., Torres-Suarez, A.I. CBD loaded microparticles as a potential formulation to improve paclitaxel and doxorubicin-based chemotherapy in breast cancer. *Int. J. Pharmaceut.* 574 (2020) # 118916, 1-12.
- Fredenberg, S., Wahlgren, M., Reslow, M., Axelsson, A. The mechanisms of drug release in poly (lactic-co-glycolic acid)-based drug delivery systems—a review, *Int. J. Pharmaceut.* 415 (2011) 34-52.
- Friess, W. and Schlapp, M. Release mechanisms from gentamicin loaded poly (lactic-co-glycolic acid) (PLGA) microparticles, *J. Pharm. Sci.* 91 (2002) 845-855.

- Fu, K., Pack, D.W., Klibanov, A.M., Langer, R. Visual evidence of acidic environment within degrading poly (lactic-co-glycolic acid) (PLGA) microspheres. *Pharm. Res.* 17(2000) 100-106.
- Gasmi, H., Danede, F., Siepmann, J., Siepmann, F. Does PLGA microparticle swelling control drug release? New insight based on single particle swelling studies. *J. Control. Release.* 213 (2015a) 120-127.
- Gasmi, H., Willart, J.F., Danede, F., Hamoudi, M.C., Siepmann, J., Siepmann, F. Importance of PLGA microparticle swelling for the control of prilocaine release. *J. Drug. Deliv. Sci. Technol.* 30 (2015b) 123-132.
- Gasmi, H., Siepmann, F., Hamoudi, M.C., Danede, F., Verin, J., Willart, J.F., Siepmann, J. Towards a better understanding of the different release phases from PLGA microparticles: Dexamethasone-loaded systems. *Int. J. Pharmaceut.* 514 (2016) 189-199.
- Grizzi, I., Garreau, H., Li, S., Vert, M. Hydrolytic degradation of devices based on poly (dl-lactic acid) size-dependence. *Biomaterials.* 16 (1995) 305–311.
- Huang, X. and Brazel, C. On the importance and mechanisms of burst release in matrix-controlled drug delivery systems. *J. Control. Release.* 73 (2001) 121-136.
- Huang, J., Mazzara, J.M., Schwendeman, S.P., Thouless, M.D. Self-healing of pores in PLGAs, *J. Control. Release.* 206 (2015) 20-29.
- Ibrahim, M.A., Ismail, A. Fetouh, M.I., Goepferich, A. Stability of insulin during the erosion of poly (lactic acid) and poly (lactic-co-glycolic acid) microspheres, *J. Control. Release.* 106 (2005) 241-252.
- Jiang, W., Gupta, R.K., Deshpande, M.C., Schwendeman, S.P. Biodegradable poly(lactic-co-glycolic acid) microparticles for injectable delivery of vaccine antigens, *Adv. Drug Deliv. Rev.* 57 (2005) 391-410.

- Kang, J. and Schwendeman, S.P. Pore closing and opening in biodegradable polymers and their effect on the controlled release of proteins. *Mol. Pharm.* 4 (2007) 104-118.
- Klose, D., Siepmann, F., Elkharraz, K., Krenzlin, S., Siepmann, J. How porosity and size affect the drug release mechanisms from PLGA-based microparticles. *Int. J. Pharmaceut.* 314 (2006) 198-206.
- Liu, J., Ren, H., Xu, Y., (...) Li, X. Mechanistic Evaluation of the Opposite Effects on Initial Burst Induced by Two Similar Hydrophilic Additives From Octreotide Acetate–Loaded PLGA Microspheres, *J. Pharm. Sci.* 108 (2019a) 2367-2376.
- Liu, J., Xu, Y., Liu, Z., Ren, H., Meng, Z., Liu, K. (...) Li, X. A modified hydrophobic ion-pairing complex strategy for long-term peptide delivery with high drug encapsulation and reduced burst release from PLGA microspheres, *Eur. J. Pharm. Biopharm.* 144 (2019b) 217-229.
- Liu, J., Xu, Y., Wang, Y. (...) Li, X. Effect of inner pH on peptide acylation within PLGA microspheres, *Eur. J. Pharm. Sci.* 134 (2019c) 69-80.
- Luan, X. and Bodmeier, R. Modification of the tri-phasic drug release pattern of leuprolide acetate-loaded poly (lactide-co-glycolide) microparticles. *Eur. J. Pharm. Biopharm.* 63 (2006) 205-214.
- Mylonaki, I., Allemann, E., Delie, F., Jordan, O. Imaging the porous structure in the core of degrading PLGA microparticles: the effect of molecular weight, *J. Control. Release.* 286 (2018) 231-239.
- Nanaki, S., Barmapalexis, P., Iatrou, A. (...) Bikiaris, D.N. Risperidone controlled release microspheres based on poly(lactic acid)-poly(propylene adipate) novel polymer blends appropriate for long acting injectable formulations, *Pharmaceutics.* 10(3) (2018) 130

- Pradal, J., Zuluaga, M.F., Maudens, P., Waldburger, J.M., Allemann, E. Intra-articular bioactivity of a p38 MAPK inhibitor and development of an extended-release system, *Eur. J. Pharm. Biopharm.* 93, (2015) 110-117.
- Riehl, M., Harms, M., Hanefeld, A., Maeder, K. Investigation of the stabilizer elimination during the washing step of charged PLGA microparticles utilizing a novel HPLC-UV-ELSD method, *Eur. J. Pharm. Biopharm.* 94 (2015) 468-472.
- Ruan, S., Gu, Y., Liu, B., (...) Cai, T. Long-Acting Release Microspheres Containing Novel GLP-1 Analog as an Antidiabetic System, *Mol. Pharm.* 15(7) (2018) 2857-2869
- Schaedlich, A., Kempe, S., Maeder, K. Non-invasive in vivo characterization of microclimate pH inside in situ forming PLGA implants using multispectral fluorescence imaging. *J. Control. Release.* 179 (2014) 52-62.
- Siepmann, J. and Goepferich, A. Mathematical modeling of bioerodible, polymeric drug delivery systems. *Adv. Drug Deliv. Rev.* 48 (2001) 229-247.
- Tamani, F., Bassand, C., Hamoudi, M.C., Danede, F., Willart, J.F., Siepmann, F. Siepmann, J. Mechanistic explanation of the (up to) 3 release phases of PLGA microparticles: Diprophylline dispersions, *Int. J. Pharmaceut.* 572 (2019a) 118819, 1-14.
- Tamani, F., Hamoudi, M.C., Danede, F., Willart, J.F., Siepmann, F. Siepmann, J. Towards a better understanding of the release mechanisms of caffeine from PLGA microparticles, *J. Appl. Polym.* 137 (2019b) 48710, 1-12.
- Tamani, F., Bassand, C., Hamoudi, M.C., Siepmann, F. Siepmann, J. Diprophylline release from PLGA microparticles: Impact of the drying-process and in vitro drug release conditions, *submitted*.
- Von Burkersroda, F., Schedl, L., Goepferich, A. Why degradable polymers undergo surface erosion or bulk erosion. *Biomaterials.* 23 (2002) 4221-4231.

- Wang, J., Helder, L., Shao, J. (...) Yang, F. Encapsulation and release of doxycycline from electrospray-generated PLGA microspheres: Effect of polymer end groups. *Int. J. Pharmaceut.* 564 (2019a) 1-9.
- Wang, T., Xue, P., Wang, A. (...) Liang, R. Pore change during degradation of octreotide acetate-loaded PLGA microspheres: The effect of polymer blends, *Eur. J. Pharm. Biopharm.* 138 (2019b) 104990.
- Wang, T., Zhang, C., Zhong, W. (...) Liang, R. Modification of Three-Phase Drug Release Mode of Octreotide PLGA Microspheres by Microsphere-Gel Composite System, *AAPS. PharmSciTech.* 20(6) (2019c) 228.

## Figure captions

- Fig. 1: SEM pictures of surfaces (lower, medium and higher magnification) of diprophylline-loaded PLGA microparticles before and after exposure to phosphate buffer pH 7.4 (“large” microparticles:  $296 \pm 95 \mu\text{m}$ , treated as for drug release studies from *ensembles* of microparticles) at 20 °C (80 rpm). The exposure times are indicated on the left-hand side. Note that the microparticles were freeze-dried after exposure to the release medium.
- Fig. 2: Impact of the temperature on diprophylline release from *ensembles* of PLGA microparticles in phosphate buffer pH 7.4. Note that the systems were agitated at 20 and 37 °C, but not at 4 °C. Three microparticle batches with different mean particle sizes (indicated in the diagram +/- SD) were studied. The results obtained at 37 °C are reproduced from (Tamani et al., 2019a), with permission. Mean values +/- SD are indicated (n = 3).
- Fig. 3: Impact of the temperature on PLGA degradation upon exposure of *ensembles* of microparticles to phosphate buffer pH 7.4. Note that the systems were agitated at 20 and 37 °C, but not at 4 °C. Three microparticle batches with different mean particle sizes (indicated in the diagram +/- SD) were studied.
- Fig. 4: Dynamic changes in the pH of the release medium upon exposure of *ensembles* of diprophylline-loaded PLGA microparticles to phosphate buffer pH 7.4 at 37, 20 and 4 °C. Note that the systems were agitated at 20 and 37 °C, but not at 4 °C. Mean values +/- SD are indicated (n = 3). Three microparticle batches with different mean particle sizes (indicated in the diagrams +/- SD) were studied.
- Fig. 5: Optical microscopy pictures of *single* diprophylline-loaded PLGA microparticles before and after exposure to phosphate buffer pH 7.4 at 20°C (80 rpm) for different



time periods (indicated at the top). The initial particle sizes are given on the left-hand side.

Fig. 6: Swelling kinetics of *single* diprophylline-loaded PLGA microparticles upon exposure to phosphate buffer pH 7.4 at 20 °C (80 rpm): Dynamic changes in the microparticles' diameter (top) and wet mass (bottom). The initial microparticle diameters are indicated in the diagrams.

Fig. 7: Drug release and swelling of *single* diprophylline-loaded PLGA microparticles upon exposure to phosphate buffer pH 7.4 at 20 °C (80 rpm). The initial microparticle diameters are indicated at the top of each diagram. The red stars highlight “sudden” partial drug release events (e.g., tiny drug crystals dissolve due to local polymer swelling and the dissolved diprophylline molecules rapidly diffuse through the swollen PLGA).

Fig. 8: Diprophylline release from *single* PLGA microparticle in phosphate buffer pH 7.4 at 20 °C (80 rpm). The initial microparticle diameters are indicated in the diagram. The red stars highlight “sudden” partial drug release events (e.g., tiny drug crystals dissolve due to local polymer swelling and the dissolved diprophylline molecules rapidly diffuse through the swollen PLGA).

Fig. 9 Schematic presentation of the hypothesized drug release mechanisms from the investigated diprophylline-loaded PLGA microparticles. Please note that the cartoons are simplifications, e.g., with respect to the homogeneity of polymer swelling. Details are explained in the text.

Fig. 10 Cartoon illustrating the root cause for the higher burst release observed with smaller microparticles compared to larger microparticles. The total surface area of many small particles is much higher than the total surface area of fewer, larger particles, resulting

in a higher probably of drug crystals having direct surface access. Details are explained in the text.

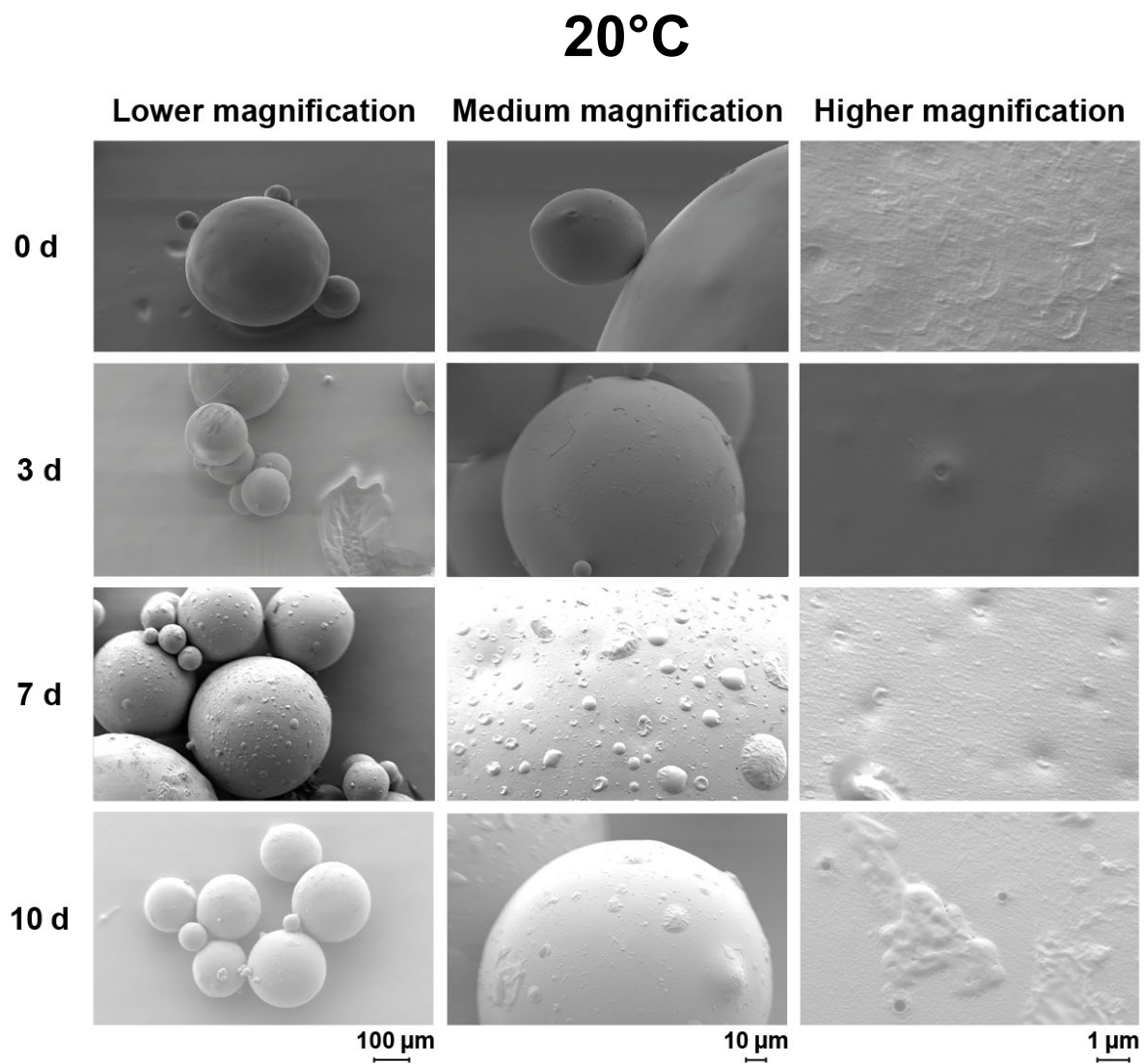


Figure 1

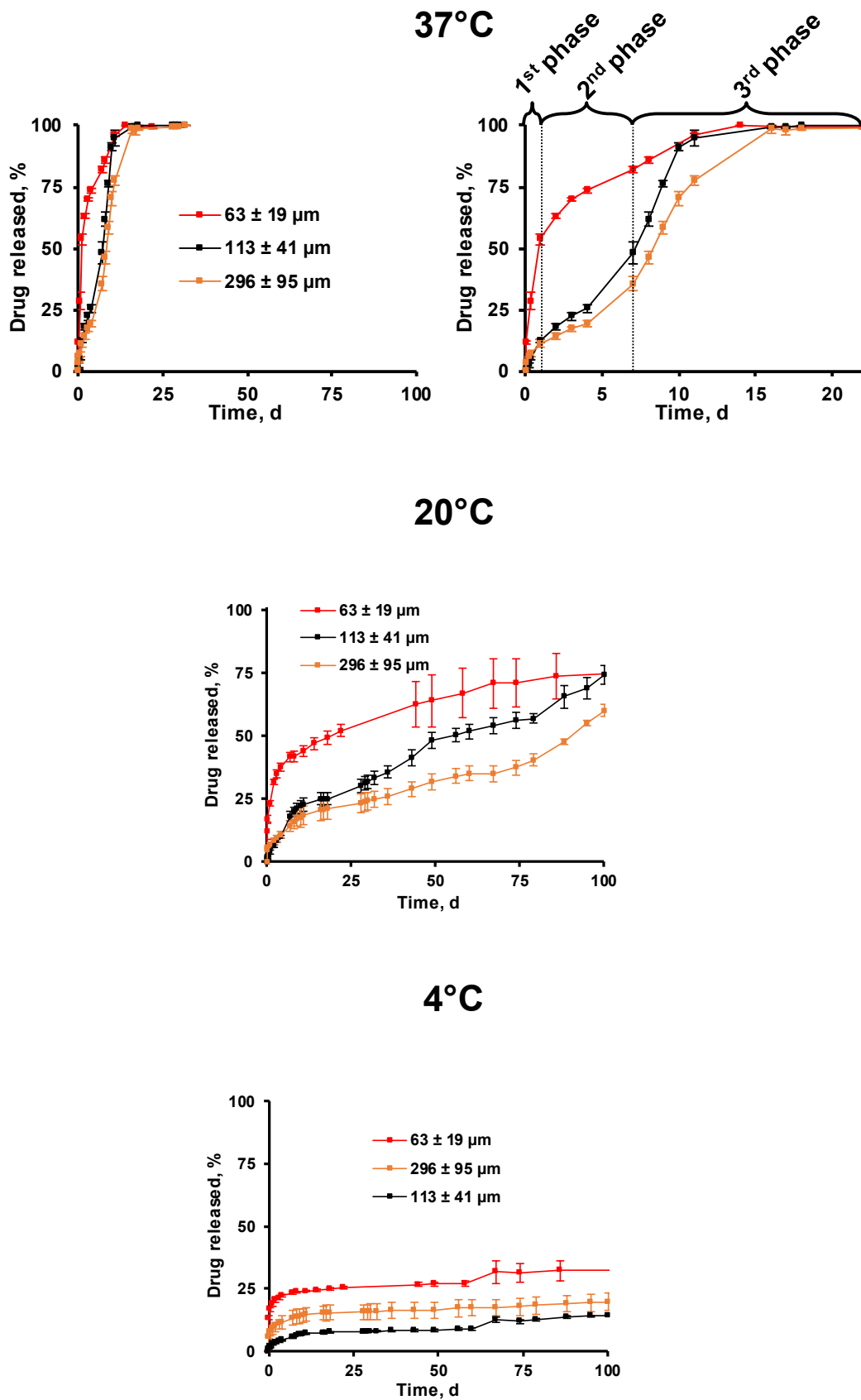


Figure 2

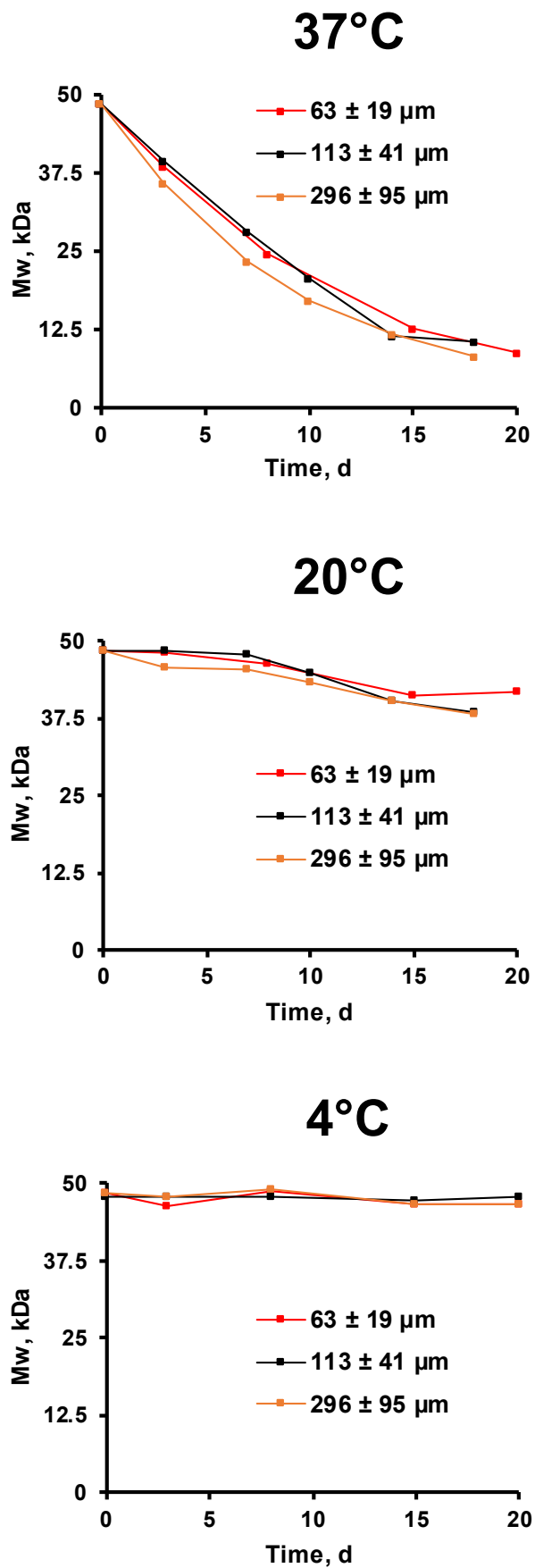


Figure 3

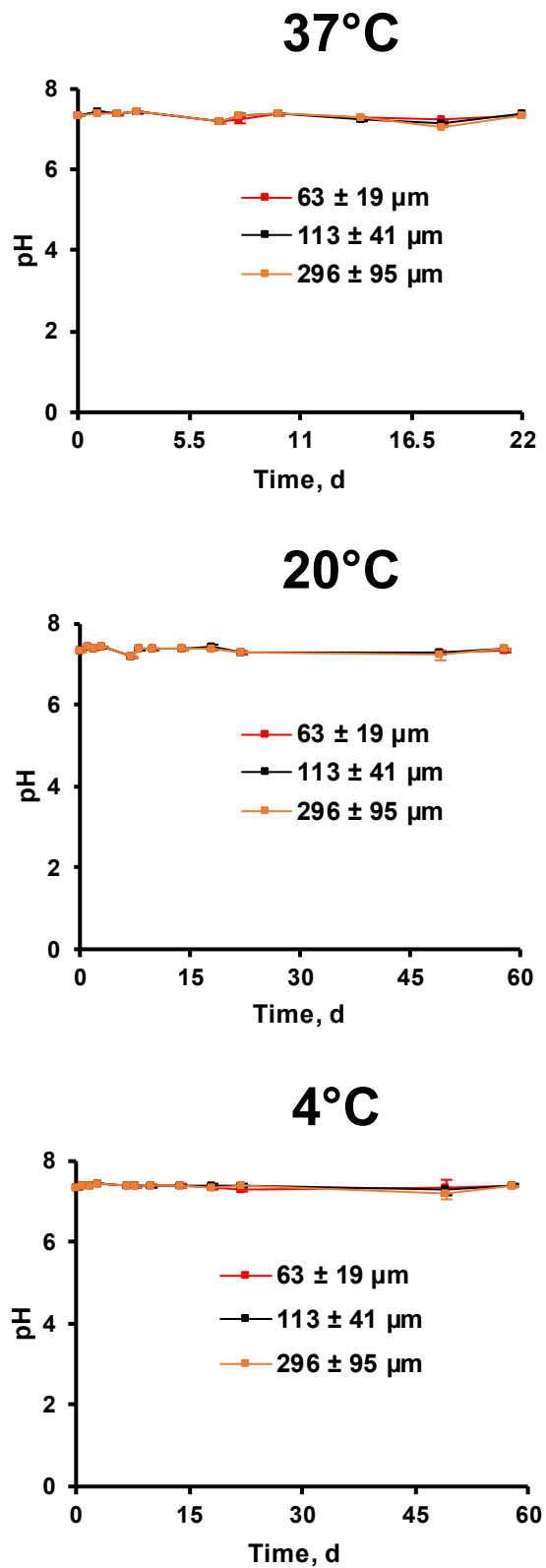


Figure 4

20°C

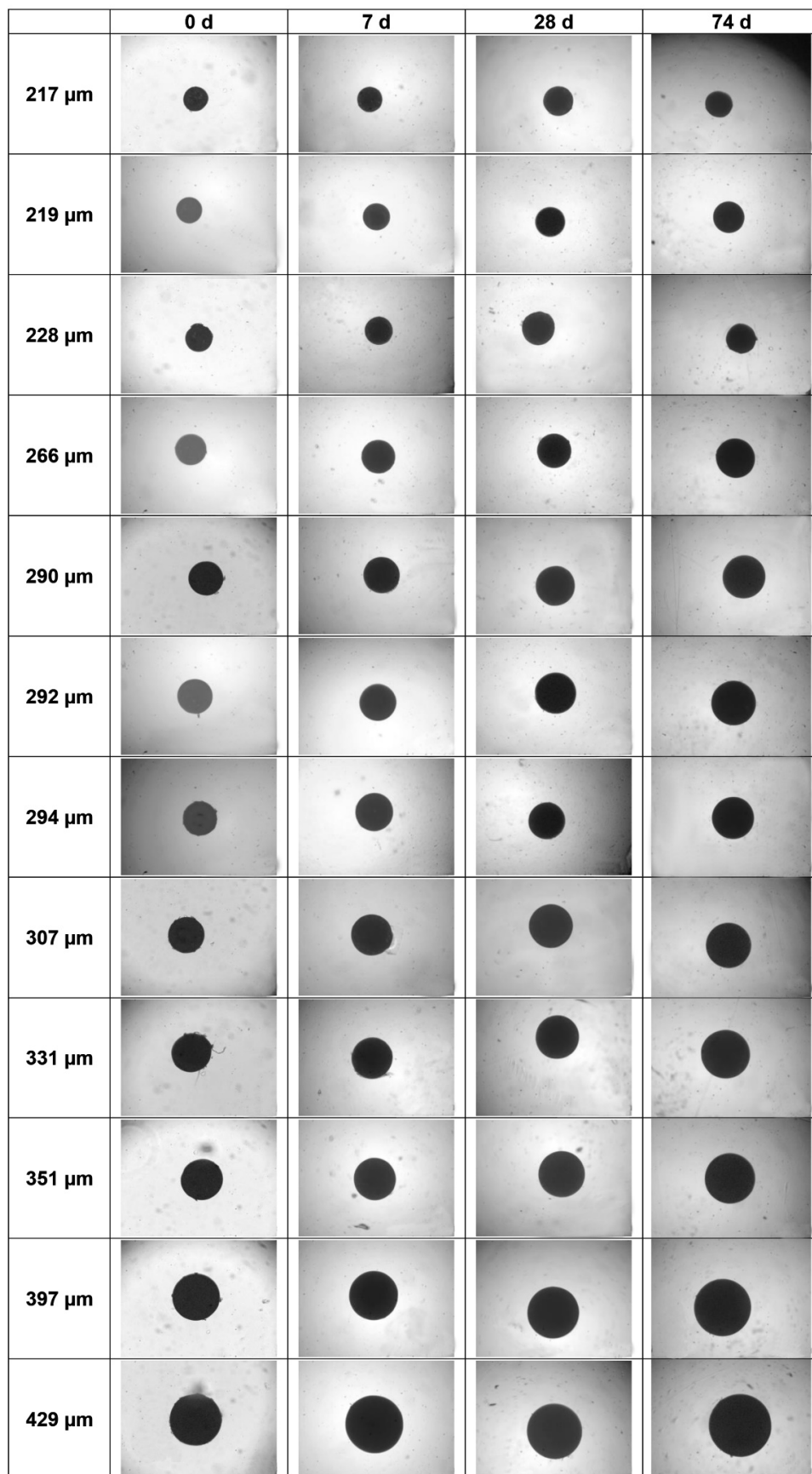
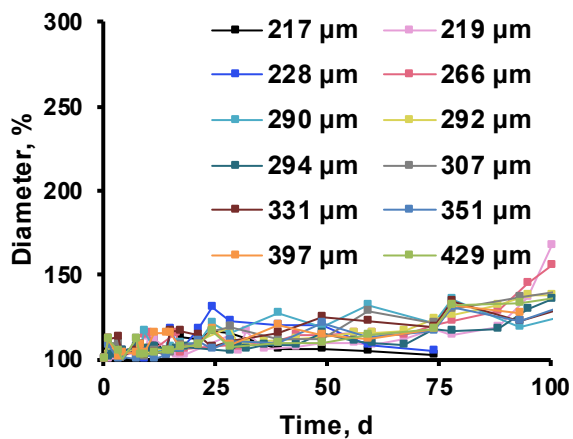
100  $\mu\text{m}$ 

Figure 5

## 20°C



## 20°C

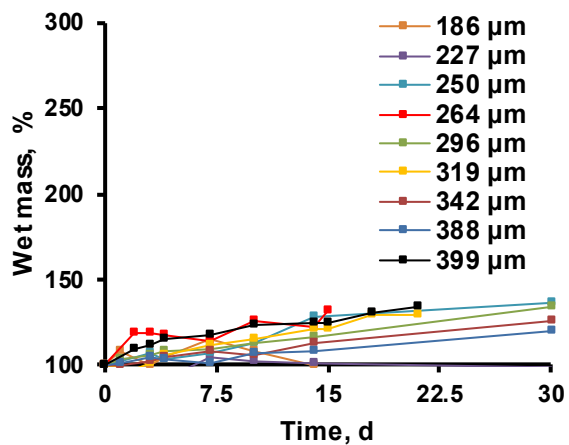


Figure 6



20°C

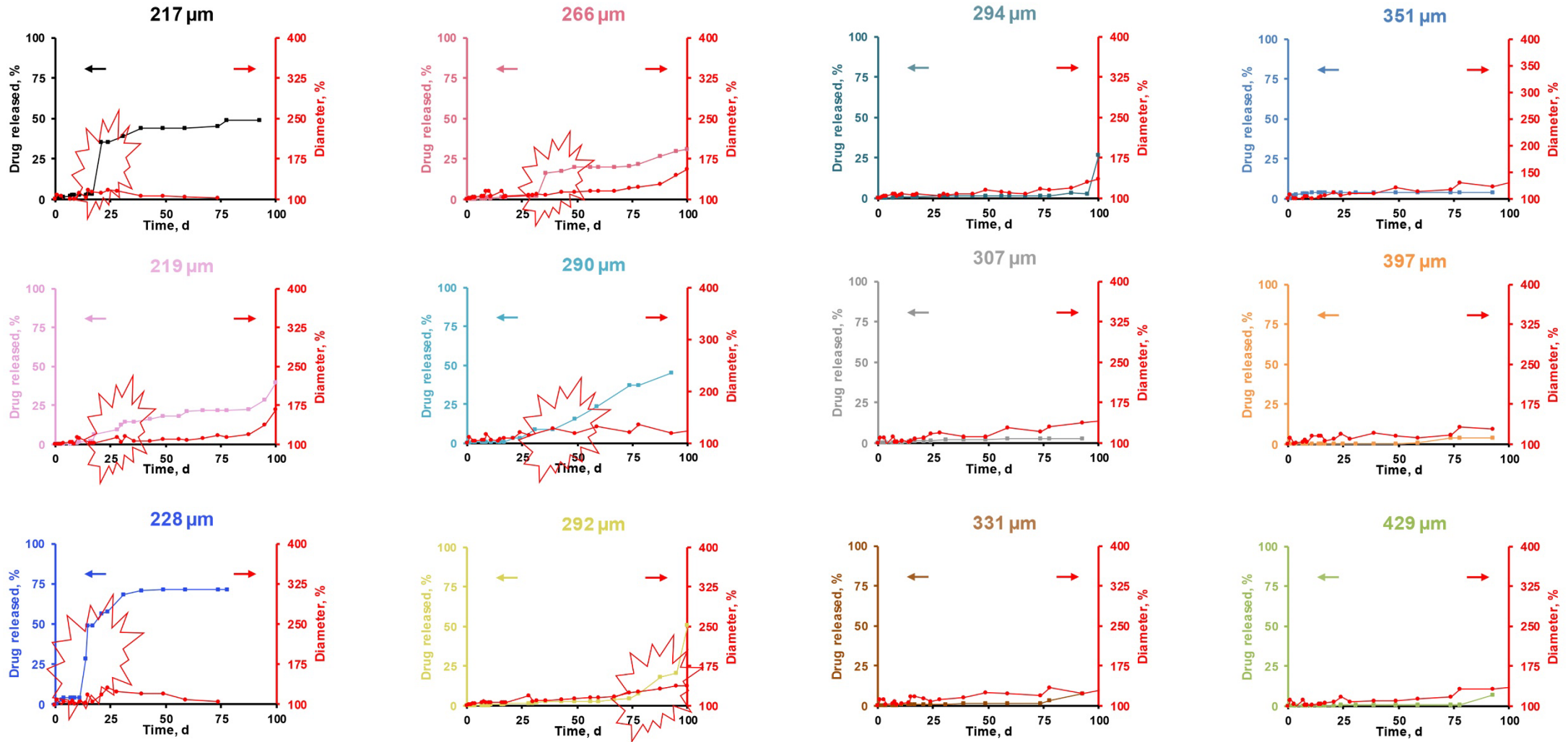


Figure 7

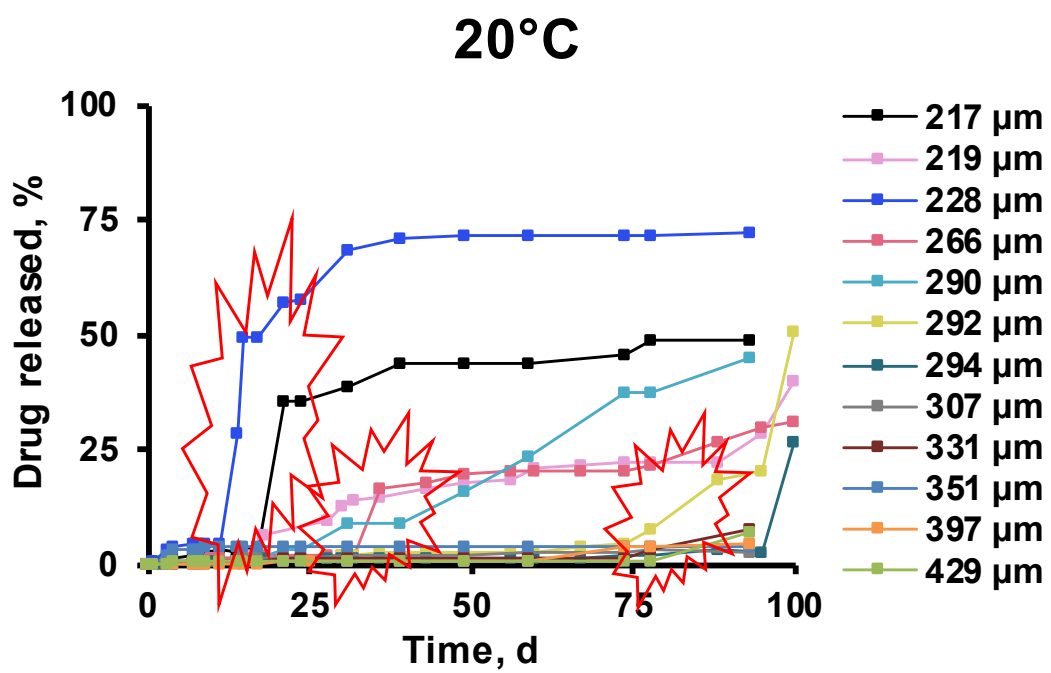
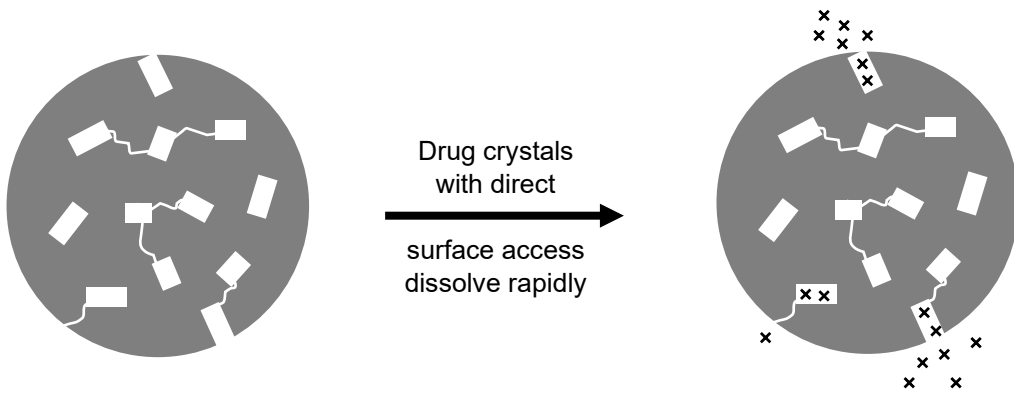
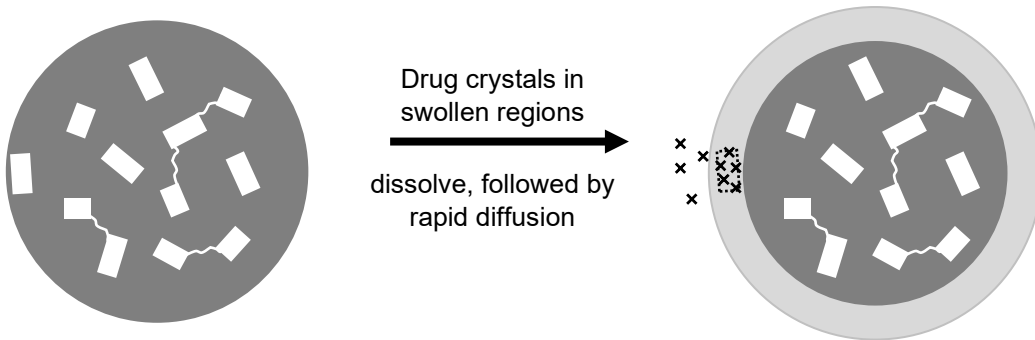


Figure 8

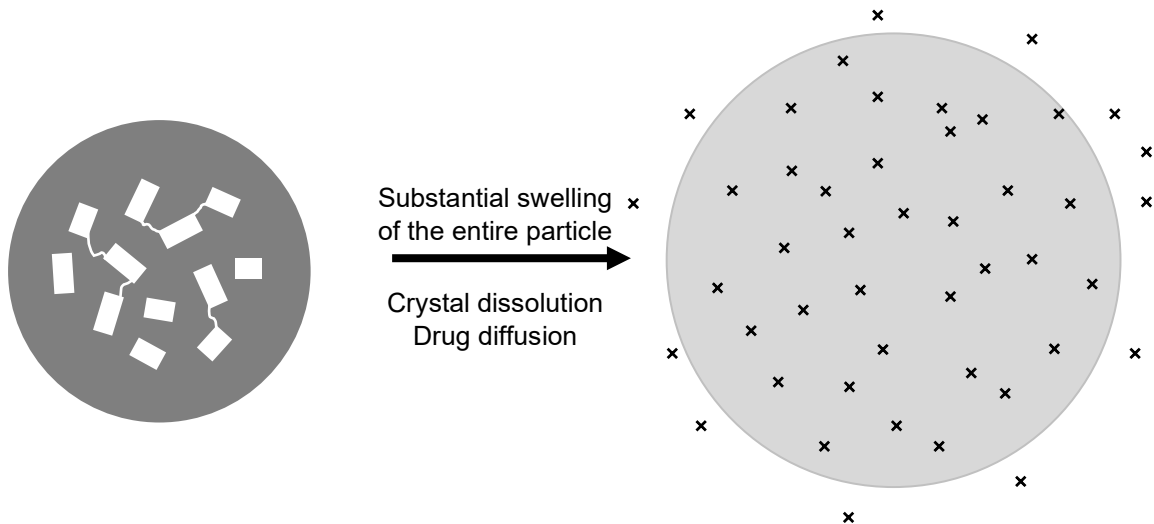
**1<sup>st</sup> Release phase (“burst release”)**



**2<sup>nd</sup> Release phase (~constant release rate)**



**3<sup>rd</sup> Release phase (again rapid, leading to complete release exhaust)**



□ Drug crystal      x x Drug molecules

Figure 9

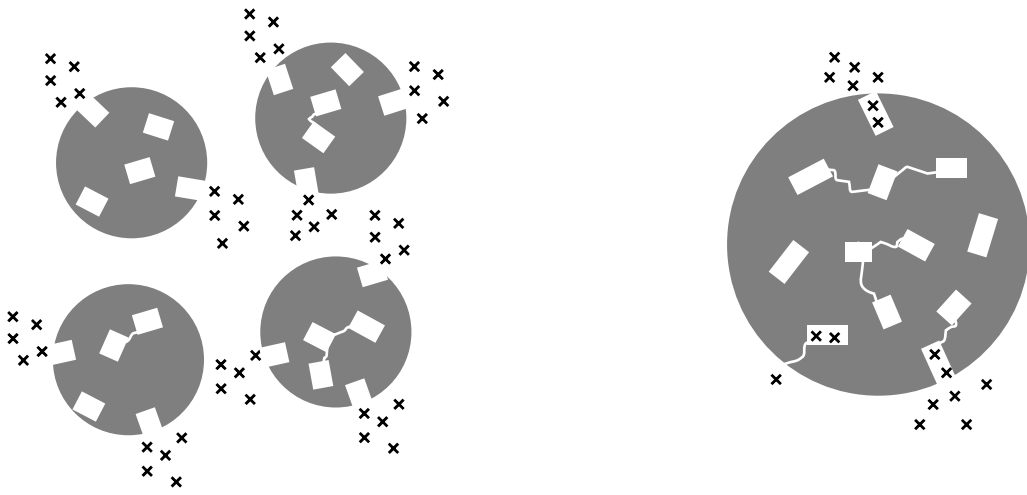


Figure 10